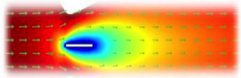
Fenómenos de Transporte

Revista Mexicana de Ingeniería Química

Vol. 12, No. 3 (2013) 527-539

NUMERICAL SIMULATION OF THE WATER SATURATION AT THE INTERFACE BETWEEN HOMOGENEOUS POROUS MEDIUM

SIMULACIÓN NUMÉRICA DE LA SATURACIÓN DEL AGUA SOBRE LA INTERFACE ENTRE MEDIOS POROSOS HOMOGÉNEOS

E. Cariaga[1], A. Vergara-Fernández[2*], M. Lévano[3] y N. Vergaray[3]

[1]*Department of Mathematical and Physical Sciences- Universidad Católica de Temuco Casilla 15D-Temuco-Chile*
[2]*Núcleo de Investigación en Energías Renovables- Universidad Católica de Temuco Casilla 15D- Temuco-Chile*
[3]*School of Informatic Engineering- Universidad Católica de Temuco Casilla 15D- Temuco-Chile*

Received December 3, 2012; Accepted October 20, 2013

Abstract

The oil-water flow in a heterogeneous porous medium was studied numerically, with special emphasis on the interface between two homogeneous layers of the porous matrix. The heterogeneity considered consists of a discontinuous capillary pressure on the interface. The differential equation was solved using a fully implicit scheme based on the upwind finite volume method. The unknown was the water saturation. This study evaluated the impact of changes in: the porosity of the entire domain, the initial water saturation, the water injection rate, the gravitational force, and the material grain size, on the water saturation at the interface. Experiments have improved the understanding of hydrodynamics on the interface. A full characterization of the porous matrix is an essential condition before defining conditions of oil extraction. The studied algorithm has great potential for use in earlier stages of design and planning for oil extraction.

Keywords: discontinuous capillary, porous medium, interface, finite volume, oil-water flow.

Resumen

En este trabajo se estudió numéricamente el flujo agua-petróleo en una medio poroso heterogéneo, con énfasis en la interface entre dos capas homogéneas de la matriz porosa. La heterogeneidad considerada consistió en una función discontinua de capilaridad sobre la interface. La ecuación diferencial fue resuelta utilizando un esquema tipo upwind completamente implícito basado en el método de volúmenes finitos. La incógnita principal fue la saturación del agua. Se evaluó el impacto sobre la saturación de la interface de diversos parámetros tales como: la porosidad, la saturación inicial de agua, la razón de inyección de agua, la fuerza gravitacional, y el tamaño del grano del material. Se concluye que una completa caracterización de la matriz porosa, junto con una adecuada combinación de parámetros de control y modelado, son condiciones fundamentales para definir condiciones de extracción adecuadas. El algoritmo estudiado posee un gran potencial para ser utilizado en etapas tempranas de diseño y planeación para la extracción del petróleo.

Palabras clave: capilaridad discontinua, medio poroso, interface, volúmenes finitos, flujo agua-petróleo.

1 Introduction

Mathematical model of immiscible two-phase flow in porous media have been applied in the oil industry to understand the movement of hydrocarbons in the subsurface (Azis and Settari, 1979; Bear, 1988; Bertsch *et al*., 2003; Salazar-Mendoza *et al*., 2004; Gerritsen and Durlofsky, 2005; Amini and Schleiss, 2009; Kinjal *et al*., 2012). Other areas of application of these models are environmental engineering (Helmig, 1997; Chen *et al*., 2006; Lee, 2010), mining (Cariaga *et al*., 2005) and nuclear energy (Hérard and Hurisse, 2009).

Heterogeneous media with different types of rock

*Corresponding author. *E-mail*: avergara@uctemuco.cl *Tel.*: +56 45 20 56 84, *Fax* +56 45 20 56 30

significantly affect the flow of the oil, and therefore, cause a decrease in the oil recovery factor. This discontinuity of physical properties can lead to oil-trapping phenomenon (Bertsch *et al*., 2003; Cancès, 2008; Cancès *et al*., 2009), which can be explained by a discontinuous capillary pressure at the interface separating the two homogeneous media. Indeed, if the mean pore radius in one media is smaller than that in the other, the oil phase must reach an entry pressure so that the oil phase can enter the less permeable media (Azis and Settari, 1979; Cancès *et al*., 2009; Enchery *et al*., 2006). Schweizer (2008) used the one-dimensional degenerate two-phase flow equations as a model for the water-drive process in oil recovery. Schweizer (2008) introduced a free boundary problem that separated the critical region with locally vanishing permeabilities from a strictly parabolic region. Additionally, Schweizer (2008) performed a rigorous derivation of the effective conservation law. In Cancès (2009) buoyancy was taken into account.

Laboratory-scale columns of porous material are frequently used in the early stages of design, to determine the numerical values of the parameters to be used in later industrial-scale designs, particularly in the oil industry and in the bioremediation of soils contaminated with hydrocarbons. For this reason, the simulations in this paper were performed in only one spatial dimension (1D) (Jiménez-Islas *et al*., 2009). A column of porous material, consisting of two homogeneous media (each fully oil saturated) has been considered; water was injected at a constant rate at the upper column boundary, so as oil could flow freely at the lower column boundary. Fig. 1 shows a schematic pore-scale considering an average value of porosity in the column where hierarchy of penetration of pores by freely imbibing water, where usually the narrowest pore is invaded first at a node of the network and penetration into the large pores awaits complete penetration of the narrowest pore. Initially, the entire porous medium is partially saturated with oil. The focus of this research is to improve our understanding of the evolution water saturation on the interface.

The mathematical model is a continuity equation for the water phase, coupled with Darcy's law (Bear, 1988). Cancès *et al*. (2009) introduced a new mathematical formulation to establish the discontinuity at the interface, which was more general than the condition used by Enchery *et al*. (2006). The interface condition applied in this work follows the formulations of Enchery *et al*. (2006) and Cancès *et al*. (2009), which are equivalent to extended capillary pressure condition of van Duijn *et al*. (1995).

The oil-trapping phenomenon has been modeled using several numerical methods (Cancès *et al*., 2009; Enchery *et al*., 2006; Ersland *et al*., 1998; Bastian and Helmig, 1999; Mikyška *et al*., 2009). Ern *et al*. (2010) designed and studied a sequential discontinuous Galerkin method to approximate two-phase immiscible incompressible flows in heterogeneous porous media with discontinuous capillary pressures. With realistic parameters they consider a domain divided into five sub domains with combination fine-coarse-fine-coarse-fine structure for the porous media, but without sensitivity analysis. Hoteit and Firoozabadi (2008) propose a consistent formulation in which the total velocity was expressed in terms of the wetting-phase potential gradient and the capillary potential gradient. They combine the mixed finite element and the discontinuous Galerkin methods to solve the pressure equation and the saturation equation. The simulations in Hoteit and Firoozabadi (2008) show the significance of capillary pressure contrast in heterogeneous media. In this work, the numerical scheme is based on the 1D upwind finite volume method (Eymard *et al*., 2000). The numerical scheme is fully implicit in time, and the damped inexact Newton method was applied as it was used by Niessner *et al*. (2005). The continuous and discrete formulations are well-posed (Cancès, 2008; Cancès, 2009; Cancès *et al*., 2009; Cancès, 2010). The discrete solution converges into the unique solution to the continuous problem (Cancès, 2008; Cancès, 2009). The computer code developed in this research assesses the effect of the water saturation on the interface in areas not considered by previous works. Under these conditions, the following are simulated numerically: the water saturation in the full domain and the water saturation at the interface. Specifically, in present work the impact on the water saturation, of changes in: the porosity of the entire domain, the initial water saturation, the water injection rate, the gravitational force, and the material grain size, is evaluated.

2 Mathematical model

The heterogeneous porous column is denoted by the mathematical domain $\Omega =]-1, 1[$, which is considered to consist of two homogeneous porous media, denoted by $\Omega_1 =]-1, 0[$ and $\Omega_2 =]0, 1[$, respectively, whereas the interface separating the two homogeneous media is denoted by $\Gamma = \{0\}$. It is assumed that the material $\Omega_1 =]-1, 0[$ is coarser, and the material $\Omega_2 =$

$]0,1[$ is finer. The maximum time recorded by the simulations will be denoted by $T > 0$. An oil-water flow is considered, where both phases are assumed to be incompressible and immiscible. Additionally, both porous materials are assumed to be inert to water and oil. The conservation of each phase and the use of the generalized Darcy's law on each sub domain lead to $(x,t) \in \Omega_i \times (0,T)$; $i = 1,2$:

$$\phi_i \frac{\partial u_i}{\partial t} + \frac{\partial}{\partial x}\left[-\mu_{w,i}(u_i)\left(\frac{\partial p_{w,i}}{\partial x} - \rho_w g\right)\right] = 0 \quad (1)$$

$$\phi_i \frac{\partial (1-u_i)}{\partial t} + \frac{\partial}{\partial x}\left[-\mu_{o,i}(u_i)\left(\frac{\partial p_{o,i}}{\partial x} - \rho_o g\right)\right] = 0 \quad (2)$$

where, $\phi_i \in [0,1]$ is the porosity of porous medium Ω_i , u_i is the water saturation (and therefore $(1-u_i)$ is the oil saturation), $\mu_{\beta,i}$ is the mobility of the phase $\beta = w,o$, where w denotes water and o denotes oil, $p_{\beta,i}$ denotes the pressure of the phase β and ρ_β denotes its density, and g denotes the gravitational constant. Additionally, the capillary pressure $p_{c,i}(u,i)$ is such that $p_{c,i}(u_i) = p_{o,i} - p_{w,i}$.

Adding Eqs. (1) and (2) shows that: $\frac{\partial q_i}{\partial x} = 0$ where q_i is the total flow-rate, which is defined as:

$$q_i = -\mu_{w,i}(u_i)\left(\frac{\partial p_{w,i}}{\partial x} - \rho_w g\right) - \mu_{o,i}(u_i)\left(\frac{\partial p_{o,i}}{\partial x} - \rho_o g\right) \quad (3)$$

Note that the Darcy's law for fluid flow in porous media $v_{\beta,i} = -\mu_{\beta,i}(u_i)\left(\frac{\partial p_{\beta,i}}{\partial x} - \rho_\beta g\right)$ with $\beta = w,o$ can be written as $v_{w,i} = q_i f_i(u_i) - \frac{\partial \varphi_i(u_i)}{\partial x} - \lambda_i(u_i)(\rho_o - \rho_w)g$, for the water phase case, where $f_i(u_i) = \mu_{w,i}(u_i)/[\mu_{w,i}(u_i) + \mu_{o,i}(u_i)]$, $\lambda_i(u_i) = \mu_{w,i}(u_i)\mu_{o,i}(u_i)/[\mu_{w,i}(u_i) + \mu_{o,i}(u_i)]$, and $\varphi_i(u_i) = -\int_0^{u_i} \lambda_i(a) p'_{c,i}(a)da$. In this work we suppose that $q = q_1 = q_2$, and $q \geq 0$, that is, the fluids move from $x = -1$ to $x = 1$. Therefore, an alternative version of Eq. (1) is obtained for each of the subdomains $i = 1,2$:

$$\phi_i \frac{\partial u_i}{\partial t} + \frac{\partial}{\partial x}\left(q_i f_i(u_i) - \frac{\partial}{\partial x}\varphi_i(u_i) - \lambda_i(u_i)(\rho_o - \rho_w)g\right) = 0 \quad (4)$$

Let us now focus on the transmission conditions through the interface Γ. Let $u_{0,1}$ denote the trace of u_1 on Γ and let $u_{0,2}$ denote the trace of u_2 on Γ. Similarly, and for $\beta = w,o$, the trace of $p_{\beta,1}$ on Γ will be denoted as $p_{\beta,0,i}$.

As established by Enchery *et al.* (2006), the pressure of phase β can be discontinuous through the interface Γ in the case where this phase is missing in the upstream side. This discontinuity can be written as:

$$\mu_{\beta,1}(u_{0,1})(p_{\beta,0,1} - p_{\beta,0,2})^+ - \mu_{\beta,2}(u_{0,2})(p_{\beta,0,2} - p_{\beta,0,1})^+ \quad (5)$$

where $y^+ = max\{y,0\}$, with y denoting an arbitrary real number. The conservation of each phase $\beta = w,o$, leads to the continuity of the fluxes at Γ (Cancès, 2008; Cancès *et al.*, 2009; Enchery, 2006).

$$v_\beta(u_{0,1}) \cdot n_1 = v_\beta(u_{0,2}) \cdot (-n_2) \quad (6)$$

where n_i denotes the outward unit normal vector to Γ. Finally, the boundary conditions are as follows: at $x = -1$ the boundary is defined as a water injection condition, that is:

$$\left(q f_1 - \frac{\partial}{\partial x}\varphi_1\right)(-1,t) = q_w \quad (7)$$

where $0 \leq q_w \leq q$. At $x = 1$ we choose to take:

$$\frac{\partial}{\partial x}\varphi_2(u_2)(1,t) = 0 \quad (8)$$

In conclusion of this section, the mathematical model is given by the nonlinear differential equation given by Eq. (4), conditions at the interface given by the Eqs. (5) and (6), the boundary conditions given by Eqs. (7) and (8), and the initial condition $u_0 = u(x,0)$, where the unknowns are u_i , and $u_{0,i}$, for $i = 1,2$. Note that this is an evolutionary problem with non-linear convective and diffusive terms. The model assumes that in the convective term, the total flow is known. Additionally, the equation could become degenerate (the diffusive term becomes zero) if $u = 0$.

3 Numerical model

The mathematical model was solved by the finite volume method in 1D. Specifically, we used a fully implicit scheme in time and an upwind type approximation for the convective term. An implicit scheme does not require a CFL (Courant, Friedrich, Levy) condition. In the process of oil extraction the spatial and temporal dimensions of the process are very large, making it inadvisable to use numerical schemes that have restrictions on the step sizes in time and space, as with explicit schemes. The discrete unknowns are also denoted as u_i, and $u_{0,i}$, for $i = 1,2$. Furthermore, to simplify the notation, we considered a uniform spatial discretization. Let $N, M \in \{1,2,3,...\}$ and $n \in \{0,1,2,...,M\}$ for which the spatial step 1 size is defined as $\delta x = 1/N$ and the temporal size step is defined as $\delta t = T/M$, $t_n = nT/M$, $x_j = j/N$, $j \in [-N,N]$, and $x_{j+1/2} = (j+1/2)/N$, $j \in [-N,N-1]$.

With these elements, the discretization of Eq. (4) with $j \in [-N, N-1]$, $n \in [0, M-1]$ is given by:

$$\phi_i \frac{u^{n+1}_{j+1/2} - u^n_{j+1/2}}{\delta t}\delta x + F^{n+1}_{j+1} - F^{n+1}_j = 0 \qquad (9)$$

where F^{n+1}_j is an approximation of the average flow through x_j during the time interval $]t_n, t_{n+1}[$ given by:

$$F^{n+1}_j := q^{n+1} f_i(u^{n+1}_{j-1/2}) - \frac{\varphi_i(u^{n+1}_{j+1/2}) - \varphi_i(u^{n+1}_{j-1/2})}{\delta x} - \lambda_i(u^{n+1}_{j-1/2})(\rho_o - \rho_w)g \qquad (10)$$

Note that in Eq. (10) the function f_i is evaluated in $u^{n+1}_{j-1/2}$ because we assume that $q \geq 0$ and use an upwind scheme for the convection. A second-order scheme for the diffusive part is applied, whereas a first-order scheme for the convection part is used. For an arbitrary function z, the notation $z^{n+1} := \frac{1}{\delta t}\int_{t^n}^{t^{n+1}} z(t)dt$ is being used.

The discrete version of the boundary conditions (7) and (8) is given by:

$$F^{n+1}_{-N} = q^{n+1}_w \qquad (11)$$

$$F^{n+1}_N = q^{n+1} f_2(u^{n+1}_{N-1/2}) - \lambda_i(u^{n+1}_{N-1/2})(\rho_o - \rho_w)g \qquad (12)$$

The discrete version of the interface condition given in Eq. (6) is given by:

$$q^{n+1} f_1(u^{n+1}_{-1/2}) - \frac{2(\varphi_1(u_{0,1}) - \varphi_1(u^{n+1}_{-1/2}))}{\delta x} - \lambda_1(u^{n+1}_{-1/2})(\rho_o - \rho_w)g = q^{n+1} f_2(u^{n+1}_{0,2}) - \frac{2(\varphi_2(u^{n+1}_{1/2}) - \varphi_2(u^{n+1}_{0,2}))}{\delta x} - \lambda_2(u^{n+1}_{0,2})(\rho_o - \rho_w)g \qquad (13)$$

which similarly defines the discrete version of the interface condition given in Eq. (5). Note that in Eq. (13) the function f_1 is evaluated in $u^{n+1}_{-1/2}$ and f_2 in $u^{n+1}_{0,2}$, because we assume that $q \geq 0$ and an upwind scheme for the convection is applied.

The discrete interface unknowns $u_{0,1}$ and $u_{0,2}$ are both defined on the interface Γ. One of the primary objectives of this study is to simulate both values, i.e., to characterize the evolution of the water saturation at the interface. The nonlinear algebraic system, formed by Eqs. (9)-(13), was solved by the damped inexact Newton-Raphson method as shown in Niessner *et al.* (2005). An adaptive selection was applied regarding the time step δt.

4 Results and discussion

The water is injected at the upper boundary $x = -1$ whereas both phases can flow freely at the lower boundary $x = 1$ (Fig. 1). Eqs. (4)-(8) were reduced to a non-dimensional form. The porosity and the mobility is the same for both sub domains, unlike capillary pressure which is considered differently (Table 1). Note that the values presented in Table 1 are dimensionless. The methodology used in this work for the computational experiments, the numerical values for the parameters, and functional expressions for mobilities have been previously applied by Cancès (2008), Ern *et al.* (2010) and Hoteit and Firoozabadi (2008). Specifically, and for reasons of computational simplicity, for the mobility function $\mu_{\beta,i}$, $\beta = w, o$; $i = 1, 2$, a generic quadratic function was used, which made it unnecessary to assign a specific numerical value to the absolute permeability.

The simulations were carried out using a linear function for the capillary pressure, given by, $p_c(u) = b - au$, with $a, b > 0$. On this note that this linear expression can be viewed as a linear version (after applying log) from the general expression Brooks-Corey (Bear, 1988; Helmig, 1997; Hoteit and Firoozabadi, 2008): $p_c(u) = p_d u^{-1/\lambda_{bc}}$, where p_d is the threshold (or entry) capillary pressure, and usually, $0.2 < \lambda_{bc} < 3.0$, where a very small λ_{bc} describes a single material grain size, while a very large λ_{bc} indicates a highly non-uniform material (Helmig, 1997). Therefore, in the simulations (cf. section 4.2.4) the slope a can be interpreted as $a = 1/\lambda_{bc}$. For this reason $0.2 < 1/a < 3.0$, that is, $1/3 < a < 5$, and has been considered $a = 1/2$ as the reference value. Linear functions for capillary pressure was applied in Cancès (2008), Helmig (1997), and Kinjal *et al.* (2012), for example. Some reference parameters values are unrealistic (porosity equal to one, for example). However, the simulations were executed using realistic values taken from a neighborhood of the reference values. The objective of the experiments was to evaluate: the impact of gravitational the term (section 4.1 versus section 4.2), the porosity (section 4.2.1), the initial water saturation (section 4.2.2), the total flow-rate and inflow of water phase (section 4.2.3), and the capillary pressure (section 4.2.4).

Table 1. Functions and reference values used for the simulations ($i = 1, 2$).

Name	**Symbol**	**Value**
Porosity of Ω_i	ϕ_i	1
Slope in capillary pressure	a	1/2
Intercept in capillary pressure $p_{c,1}$	b_1	2
Intercept in capillary pressure $p_{c,2}$	b_2	3
Capillary pressure in Ω_i	$p_{c,i}(u)$	$b_i - au$
Water mobility in Ω_i	$\mu_{w,i}(u)$	u^2
Oil mobility in Ω_i	$\mu_{o,i}(u)$	$(1-u)^2$
Fractional flow in Ω_i	$f_i(u)$	$\frac{u^2}{1+2u(u-1)}$
Total flow-rate	q	1
Inflow of water phase	q_w	1
Diffusion function in Ω_i	$\varphi_i(u)$	$\frac{1}{4}(\frac{u^3}{3} - \frac{u^2}{2} - \frac{u}{2} + \frac{1}{2}\tan^{-1}(2u-1)) + \frac{\pi}{32}$

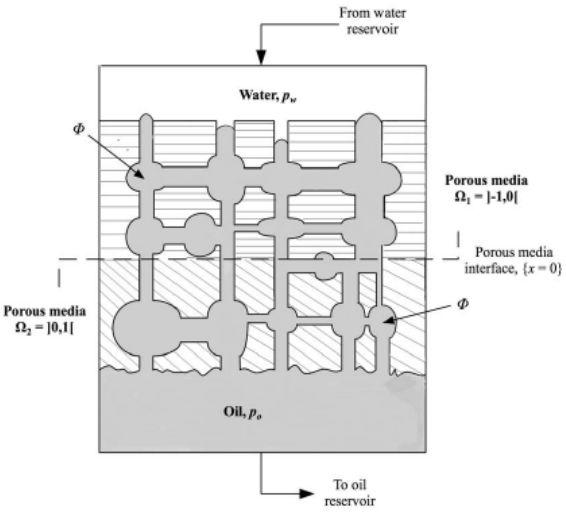

Fig. 1. Schematic of the physical model for the simulated porous medium.

The computer code was successfully validated by Cancès (2008 and 2009), that is, the convergence of numerical algorithm was proved, from theoretical point of view. By this reason, and with the objective of to check the numerical convergence (but not to estimate the rate of convergence), different spatial meshes were considered: 250, 500, 750, 1000, 1250, 1500, 1750, and 2000 nodes in the interior of $\Omega_1 =]-1,0[$. The curve of approximation of the water saturation on the left side of interface, that is, $u_{0,1}$, built with 2000 nodes and without the gravitational term, was chosen as "reference function" or "exact solution". Table 2 show the relative error computed with the norms $\|\cdot\|_p$, $p = 1, 2, +\infty$. It is clear from Table 2 that the computational code is numerically convergent.

4.1 Simulations without the gravitational term: $\lambda(u)(\rho_o - \rho_w)g$ and $u_0 = 0$ as initial condition

In this section, the numerical simulations performed for the solution of the algebraic system Eqs. (9)-(13), without gravitational term, are reported. The simulations (shown in Fig. 2a to Fig. 2d) were performed using the functions and parameters given in Table 1. In each case, the physics of the phenomenon was analyzed. Initially, the column is fully saturated with oil, i.e., $\{u_0 = 0\}$. Fig. 2a shows the water saturation in $\Omega_1 =]-1,0[$, at various time points. At $t = 0.758562[-]$ the water saturation at $\{x = 0^-\}$ is equal to 1.0, $\{u_{0,1} = 1\}$ that is, the left side of the interface does not contain oil. Fig. 2a also shows that the water front reaches the interface between $t = 0.72[-]$ and $t = 0.74[-]$. According to the capillary pressures used in the experiments, the saturation $\{u_0, 1 = 1\}$ is the threshold saturation, that is the saturation with which the entry pressure is obtained, that is, the capillary pressure needed to displace the non-wetting phase from the largest pore, which occurs at $t = 0.758562[-]$. Once the oil saturation begins to decrease on the left side of the interface $\{x = 0^-\}$, the rate of change of oil saturation in the domain $\Omega_1 =]-1,0[$ decreases. The most notable aspect of Fig. 2a is that on the left side of the interface $\{x = 0^-\}$, the oil is removed within a short time, when compared to the total simulation time, which makes it essential to use an adaptive selection for the time step. Fig. 2b shows the water saturation in $\Omega_2 =]0,1[$ at various time points. Fig. 2a shows that shortly before time $t = 0.76[-]$, the oil begins to withdraw from domain Ω_2, and Fig. 2b shows that the water saturation is stabilized at approximately 0.8,

at approximately $t = 2.00[-]$. Once the oil saturation begins to decrease at the boundary $\{x = 1\}$, the rate of change of oil saturation in the domain $\Omega_2 =]0, 1[$ decreases. From Figs. 2a and 2b, is possible to deduce that the withdrawal of oil is approximately 3% slower in $\Omega_2 =]0, 1[$ than in $\Omega_1 =]-1, 0[$. From Figs. 2a and 2b is also possible to estimate the oil recovery factor and the time needed to obtain the oil recovery factor. Fig. 2c shows the evolution of the water saturation on the left side of the interface $\{x = 0^-\}$ from $t = 0.72[-]$ to $t = 0.77[-]$. In Fig. 2c the oil begins to be withdraw from the left side of the interface is observed from time $t = 0.73[-]$, and the oil is completely withdrawn shortly before $t = 0.76[-]$, specifically at $t = 0.758562[-]$, as in Fig. 2a. Note that the filling of water (draining of oil) on the left side of the interface $\{x = 0^-\}$ takes approximately 4%, in proportion to $t = 0.758562[-]$ when $u_{01} = 1$. This percentage is similar to that estimated for the difference between the oil withdrawal rates between the homogeneous sub-domains $\Omega_1 =]-1, 0[$ and $\Omega_2 =]0, 1[$, which gives rise to the conjecture that the time needed to overcome the discontinuity in the capillary pressure at the interface is significant in proportion to the time when $u_{01} = 1$. Fig. 2d shows the evolution of the water saturation on the right side of the interface $\{x = 0^+\}$ from time $t = 0.75[-]$ to $t = 0.80[-]$. The evolution of the water saturation on the two sides of the interface is very different. Indeed, according to Fig. 2c, the oil is quickly flushed from the left side $\{x = 0^-\}$, whereas on the right side $\{x = 0^+\}$, the oil is not completely withdrawn, and withdraws at a lower rate, and the water saturation is stabilized approximately 0.8 (Fig. 2b). This difference in the saturation curves on both sides of the interface can be explained by the lower permeability of oil in the sub-domain $\Omega_2 =]0, 1[$.

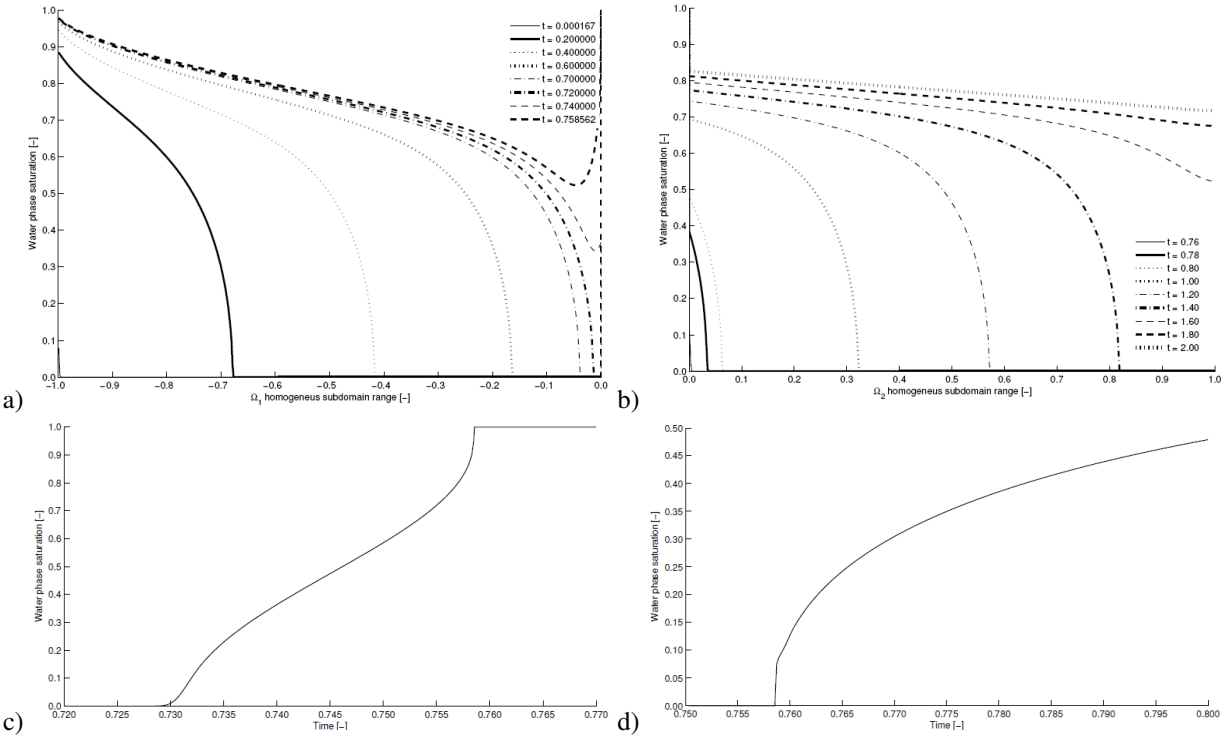

Fig. 2. Water saturation curves (without gravitational term): (a) in the sub-domain $\Omega_1 =]-1, 0[$, (b) in the sub-domain $\Omega_2 =]0, 1[$, (c) on the left side of the interface $\{x = 0^-\}$, (d) on the right side of the interface $\{x = 0^+\}$.

Table 2. Relative error with respect to $u_{0,1}$ computed with 2000 nodes.

Number of nodes	$\|\cdot\|_1$	$\|\cdot\|_\infty$	$\|\cdot\|_2$
250	0.269354	0.254267	0.245188
500	0.113442	0.169730	0.115390
750	0.062294	0.130614	0.067469
1000	0.037086	0.102153	0.042136
1250	0.021885	0.062320	0.025037
1500	0.011835	0.022437	0.012999
1750	0.005018	0.009583	0.005505
2000	0.000000	0.000000	0.000000

4.2 Simulations with the gravitational term: $\lambda(u)(\rho_o - \rho_w)g$ and $u_0 = 0.01$ as initial condition

In this section, the numerical simulations performed for the solution of the algebraic system Eqs. (9)-(13), with gravitational term, are reported. The simulations (shown in Fig. 3a to Fig. 7c) were performed using the functions and parameters given in Table 1. In each case, the physics of the phenomenon was analyzed. Fig. 3a shows the water saturation evolution on the sub domain $\Omega_1 =]-1, 0[$ from $t = 0.000167$ to $t = 0.556730$. Through the comparison of Figs. 2a and 3a it shows that oil recovery is faster with the gravitational term. Furthermore, the water saturation in the left side of the interface increases its value virtually from the beginning due mainly to the presence of gravitational term. Figs. 3b and 3c show the evolution of water saturation on the interface (from left and right respectively) with and without gravitational term. Fig. 3c shows that the non-inclusion of gravity in the mathematical model could lead to an overestimation of the recovery factor. This section ends with Fig. 3d showing the simultaneous evolution of water saturation at the interface.

4.2.1 Effect of the initial condition on the water saturation at the interface

Fig. 4 shows the evolution of water saturation on the left side of the interface for different values of the initial saturation of the porous medium. It is noted that an increase in initial water saturation of the porous medium involves a faster increase of saturation on the left side of the interface. Fig. 4 suggests that an increase in the initial water saturation could produce a faster oil recovery, but not necessarily a greater amount of oil.

4.2.2 Effect of the porosity on the water saturation at the interface

Fig. 5a shows the water saturation on the left side of the interface $\{x = 0^-\}$ for different and realistic values of the porosity: $\phi = 0.2, 0.4, 0.6, 0.8, 1.0$. It has been considered a porosity value equal to one in order to illustrate and establish the extreme behavior on this parameter. A decrease in porosity results in the left side of the interface becoming fully saturated in less time. This decrease is due to the variation in the available empty space that will be occupied by water, i.e., the lower porosity increases the fluid rate inside the porous medium, and the oil phase moves more quickly through porous medium. This is valid under the assumption that the porous structures studied are consistent with the pressure, that is, that the porous matrix is non-deformable in the range of pressures simulated. Note that from Fig. 5a, an increase of 0.2[-] units of porosity implies a decrease of 0.1[-] units of time required to saturate the left side of the interface with water. Fig. 5b shows the water saturation on the sub domain homogeneous $\Omega_1 =]-1, 0[$, at time $t = 0.4$, for different values of porosity. It is clearly seen that a smaller value of porosity involves faster progress wetting front and increased oil recovery. Figs. 5a and 5b illustrates the importance of properly estimate the porosity, which significantly impacts the saturation of fluid phases.

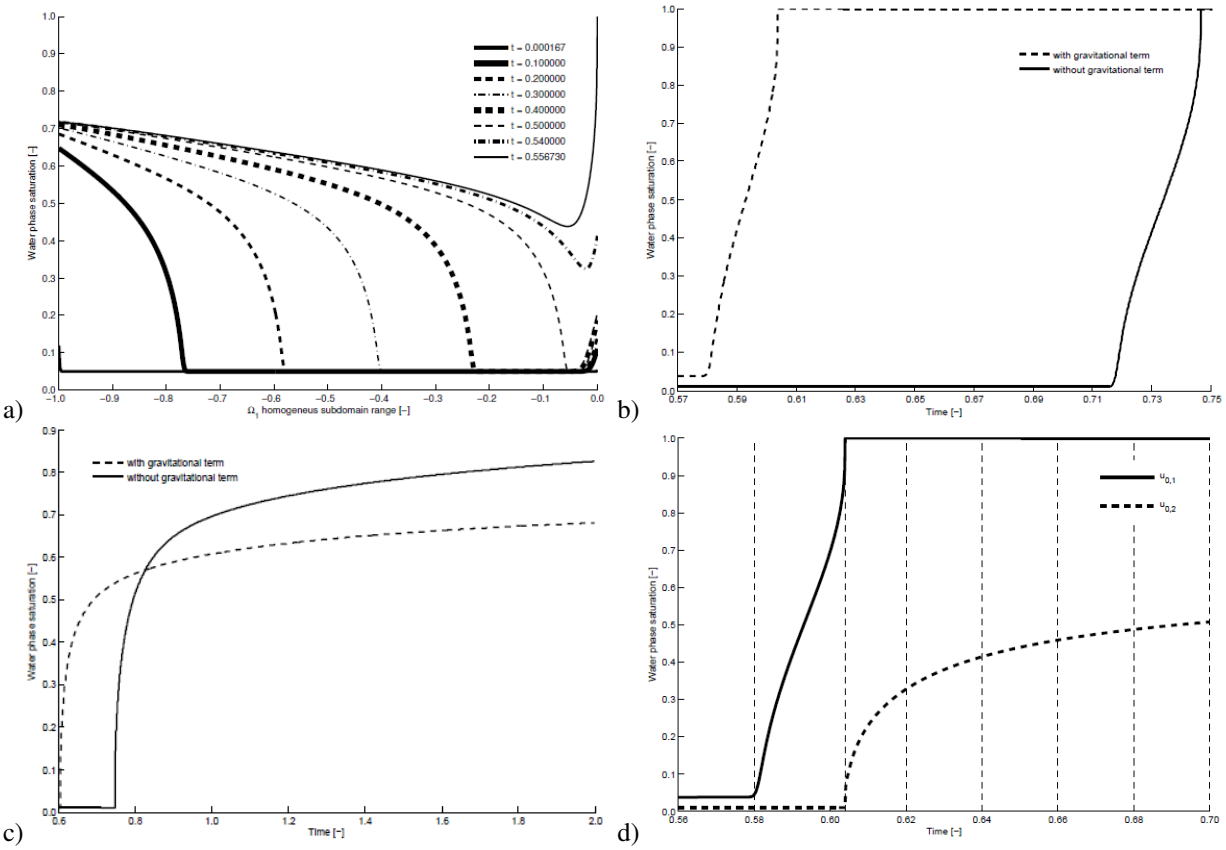

Fig. 3. Water saturation curves: (a) in the homogeneous sub-domain $\Omega_1 =]-1, 0[$, (b) on the left side of the interface $\{x = 0^-\}$, (c) on the right side of the interface $\{x = 0^+\}$, (d) on the left and the right side of the interface $\{x = 0\}$. Simulations in Figures (a) y (d) include the gravitational term.

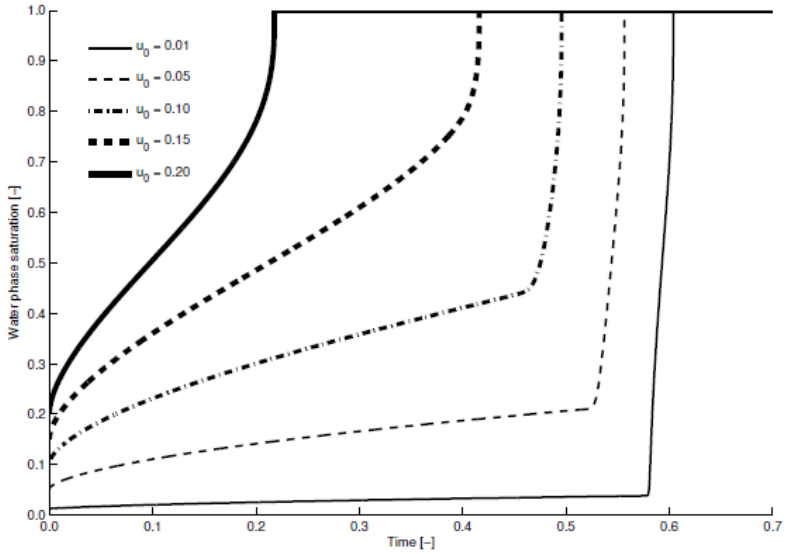

Fig. 4. Water saturation curve on the left side of the interface $\{x = 0^-\}$, at different initial condition: $u_0 = 0.01, 0.05, 0.10, 0.15, 0.20$. Simulations include the gravitational term.

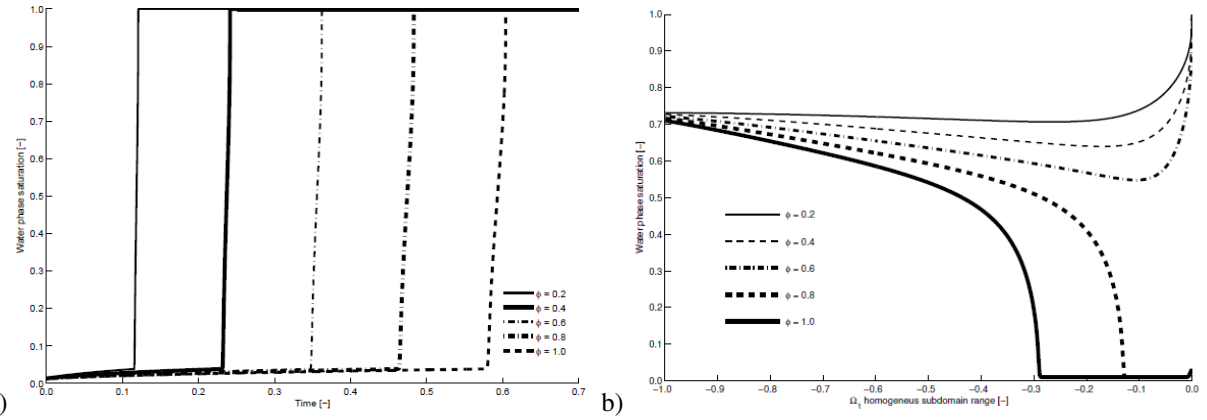

Fig. 5. Water saturation curves (with gravitational term) at different porosities values $\phi = 0.2, 0.4, 0.6, 0.8, 1.0$: (a) on the left side of the interface $\{x = 0^-\}$, (b) in the sub-domain $\Omega_1 =]-1, 0[$ and in the time $t = 0.4$.

4.2.3 Effect of the water injection rate q_w on the water saturation at the interface

In this section we evaluate the impact of a relevant control parameter such as the water injection rate q_w at the upper end of the column $\{x = -1\}$. According to van Duijn *et al*. (1995), the essential parameter that determines the amount of oil trapped is $(\sigma/v_{isw}) \cdot q_w$, where σ is the interfacial tension between the oil and water and v_{visw} is the water viscosity. In the following analysis, σ and v_{visw} are assumed to be constant. Fig. 6a shows the effect of q_w on the water saturation on left side of the interface $\{x = 0^-\}$. Fig. 6b shows the water saturation on the sub domain homogeneous $\Omega_1 =]-1, 0[$, at time $t = 0.4$, for different values of q_w. The reference value was $q_w = 1$ (Table 1). Figs. 6a and 6b shows that a decrease in q_w implies an increase in the time required to initiate the evacuation of oil on the left side of the interface, but this relationship is not linear. However, as q_w increases, at a certain value, the impact on the left side of the interface is less significant. In other words, an increase in q_w is not always justified. An important application of this computational code is the ability to evaluate several scenarios for production. For a specific example, this method could be used to determine the best value of q_w given a heterogeneous porous media such that, the oil saturation is minimal, and the process time is as short as possible.

4.2.4 Effect of the capillary pressure: $p_c(u) = b - au$, on the water saturation at the interface

The objective of this section is to evaluate the impact of grain size material on water saturation, where the Brooks-Corey parameter $\lambda_{bc} = 1/a$ represent, the grain size material in the porous matrix (Helmig, 1997). Figs. 7a and 7b shows the water saturation on the interface (left and right, respectively) for different values of the capillary pressure slope: $a = 0.5, 1.0, 2.0, 3.0, 4.0$. The value $a = 0.5$ indicates a highly non-uniform material, while the value $a = 4.0$ describes a single grain size material. The reference value for the slope was $a = 0.5$ (Table 1). Fig. 7a shows that a decrease in the slope a implies an increase in the startup time and a decrease in the time required to empty the oil from the left side of the interface $\{x = 0^-\}$. Fig. 7a also shows that an increase in the slope a implies a decrease in the startup time and an increase in the time required to empty the oil from the left side of the interface $\{x = 0^-\}$. Fig. 7a confirm, and allow us to quantify in relative terms, the importance of the capillary pressure on the ability to remove the oil from a heterogeneous porous medium.

From Fig. 7b it is observed that an increase in the value of the slope implies that the time required to reach the full saturation state is slightly lower. Fig. 7a shows that the impact of changing the capillary pressure is less significant on the right side of the interface. In the case where the porous medium is formed by a material with a more uniform grain size the water saturation increases faster on the left sub domain. However, the evolution of water saturation on the left side of the interface is slower. Conversely, if the porous material has a non-uniform grain size the evolution of water saturation is slower on the left sub domain. However, on the left side of the interface the evolution of water saturation is faster. The behavior on the left sub domain is expected, unlike what was observed in the simulations on the right side of the interface, where it notes, if you increase the value of

the slope a, the water saturation increases faster, but in the long term the recovery factor is lower. Fig. 7c shows the water saturation on the homogeneous sub domain $\Omega_1 =]-1, 0[$, at time $t = 0.4$, for different values of the slope a. The analysis from Fig. 7b is ratified by the behavior observed in Fig. 7c, that is, if the porous medium has a more uniform grain size then the water saturation increases faster, but it does not necessarily improve the recovery factor.

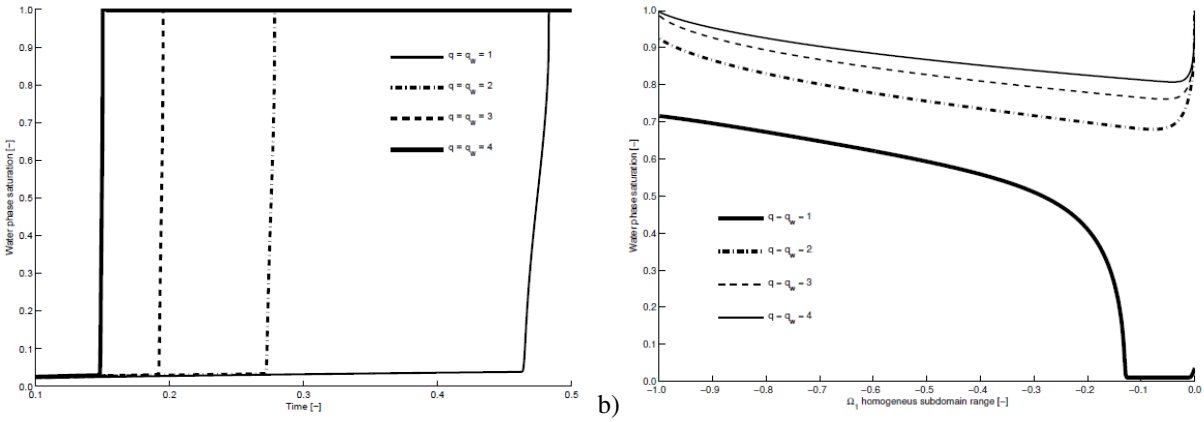

a) b)

Fig. 6. Water saturation curves (with gravitational term) at total rates flow and water injection rates: $q = q_w = 1, 2, 3, 4$: (a) on the left side of the interface $\{x = 0^-\}$, (b) in the homogeneous sub-domain $\Omega_1 =]-1, 0[$.

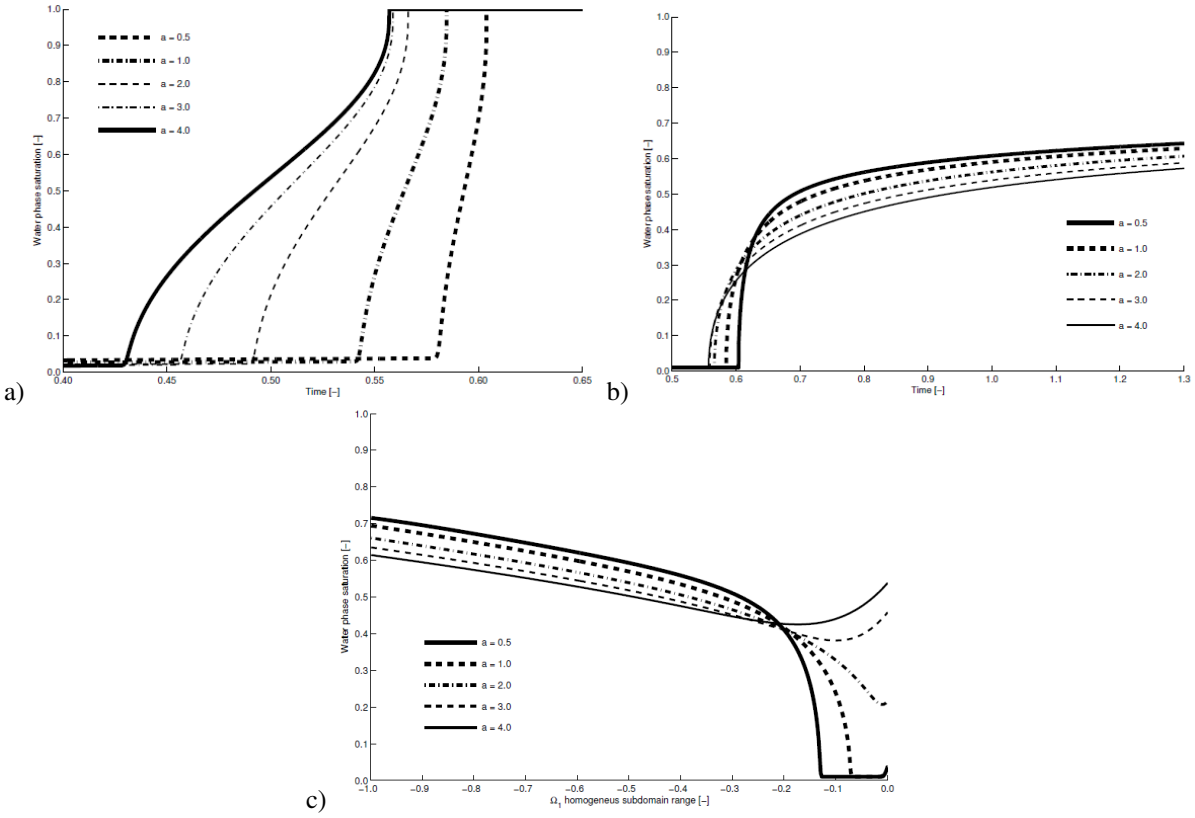

a) b) c)

Fig. 7. Water saturation curves (with gravitational term) at different capillary pressure slope $a = 0.5, 1.0, 2.0, 3.0, 4.0$: (a) on the left side of the interface $\{x = 0^-\}$, (b) on the right side of the interface $\{x = 0^+\}$, (c) in the homogeneous sub-domain $\Omega_1 =]-1, 0[$.

Conclusions

In this paper, we have considered the problem of simulating the water saturation, and by inference, oil saturation, of the interface separating two homogeneous media of the porous matrix. To accomplish this, a heterogeneous porous column composed of two homogeneous media was considered, where the interface was the main interest in this research. From a modeling point of view, the gravitational term has a high impact on all simulations performed. By another hand, a full characterization of the hydrodynamics of a porous medium is essential to simulate the oil recovery factor. In effect, in a column of porous material, small differences in the porosity and in the grain size material, that is, the Brooks-Corey parameter in the capillary pressure, can lead to large differences in the oil recovery factor. However, the impact is greater on the upstream side of the interface. The water injection rate is a very useful control parameter. A small increase in water injection rate could result in a significant increase in the oil recovery factor on both upstream and downstream sides of the interface. In this sense the evaluation of the intial condition of water saturation suggests, from numerical point of view, adding water to the system prior to the injection process itself. However, this apparent solution is not feasible because the industrial costs may be too high. Finally, the simulation of the saturation at the interface is useful for estimating the time delay in the evacuation of the oil generated by the heterogeneity. The studied algorithm has potential for use in earlier stages of design and planning for oil extraction.

Acknowledgements

EC has been supported by Fondecyt project 11100358.

Nomenclature

a	slope of capillary pressure
b	intercept of capillary pressure
g	gravitational constant
f_i	fractional flow
F_j^n	discrete flow
n_i	normal vector
n, N, M	mesh parameters
p_β	pressure of phase
p_c	capillary pressure
p_d	entry pressure
q	total flow rate
q_w	water injection rate
T	total simulation tiem
t	time
u	water saturation
$u_{0,i}$	trace of u on interface
u_0	initial condition
v_β	Darcy's velocities
v_{visw}	water viscosity
x	Cartesian coordinate
y^+	maximum between y and 0

Greeks letters

Ω	mathematical domain
Ω_i	sub domain i
Γ	interface
ϕ	porosity
μ_β	mobility of phase β
ρ_β	density of phase β
λ	gravitational function
φ	diffusion function
δt	time step
δx	spatial step
λ_{bc}	Brooks-Corey parameter
σ	interfacial tension

References

Amini, A. and Schleiss, A. (2009). Numerical modeling of oil-water multiphase flow contained by an oil spill barrier. *Engineering Applications of Computational Fluid Mechanics 3*, 207-219.

Aziz, K. and Settari, A. (1979). *Petroleum Reservoir Simulation*. Elsevier Applied Science Publishers. London.

Bastian, P. and Helmig, R. (1999). Efficient fully-coupled solution techniques for two-phase flow in porous media-Parallel multigrid solution and large scale computations. *Advances in Water Resources 23*, 199-216.

Bear, J. (1988). *Dynamics of Fluids in Porous Media*. Dover. New York.

Bertsch, M., Passo, R. and van Duijn, C. (2003). Analysis of oil trapping in porous media flow. *SIAM Journal on Mathematical Analysis 35*, 245-267.

Cancès, C. (2008). Écoulements diphasiques en milieux poreaux hétérogènes: modélisation et

analyse. *Thèse Docteur de L'Université de Provence*. Université de Provence.

Cancès, C. (2009). Finite volume scheme for two-phase flow in heterogeneous porous media involving capillary pressure discontinuities. *M2AN Mathematical Modelling and Numerical Analysis 43*, 973-1001.

Cancès, C., Gallouët, T. and Porretta, A. (2009). Two-phase flows involving capillary barriers in heterogeneous porous media. *Interfaces and Free Bound 11*, 239-258.

Cancès, C (2010). On the effects of discontinuous capillaries for immiscible two-phase flows in porous media made of several rock-types. *Networks and Heterogeneous Media 5*, 635-647.

Cariaga, E., Concha, F. and Sepúlveda, M. (2005). Flow through porous media with applications to heap leaching of copper ores. *Chemical Engineering Journal 111*, 151-165.

Chen, Z., Huan, G. and Ma, Y. (2006). *Computational Methods for Multiphase Flows in Porous Media*. Society for Industrial and Applied Mathematics (SIAM).

Correa, A. and Firoozabadi, A. (1996). Concept of gravity drainage in layered porous media. *SPE Journal March*, 101-111.

Enchery, G., Eymard, R. and Michel, A. (2006). Numerical approximation of a two-phase flow problem in a porous medium with discontinuous capillary forces. *SIAM Journal on Numerical Analysis 43*, 2402-2422.

Ern, A., Mozolevski, I. and Schuh, L. (2010). Discontinuous Galerkin approximation of two-phase flows in heterogeneous porous media with discontinuous capillary pressures. *Computer Methods in Applied Mechanics and Engineering 199*, 1491-1501.

Ersland, B., Espedal, M. and Nybo, R. (1998). Numerical methods for flows in a porous medium with internal boundary. *Computers & Geosciences 2*, 217-240.

Eymard, R., Gallouet, T. and Herbin, R. (2000). *Finite Volume Methods. Handbook of Numerical Analysis. Vol. VII*. Edited by P. G. Ciarlet and J. L. Lions. Elsevier Science B. V.

Fučik, R., Mikyška, J., Sakaki, T., Beneš, M. and Illangasekare, T. (2010). Significance of dynamic effect in capillarity during drainage experiments in layered porous media. *Vadose Zone Journal 9*, 697-708.

Gerritsen, M. and Durlofsky, L. (2005). Modeling Fluid Flow in Oil Reservoirs. *Annual Review of Fluid Mechanics 37*, 211-238.

Helmig, R. (1997). *Multiphase Flow and Transport Processes in the Subsurface: a Contribution to the Modeling of Hydrosystems*. Springer.

Helmig, R. and Huber, R. (1998). Comparison of galerkin-type discretization techniques for two-phase flow in heterogeneous porous media. *Advances in Water Resources 21*, 697-711.

Hérard, J. and Hurisse, O. (2009). Some recent numerical advances for two-phase flow modeling in NEPTUNE project. *International Journal for Numerical Methods in Fluids 59*, 285-307.

Hoteit, H. and Firoozabadi, A. (2008). Numerical modeling of two-phase flow in heterogeneous permeable media with different capillary pressures. *Advances in Water Resources 31*, 56-73.

Jiménez-Islas, H., Calderón-Ramírez, M., Navarrete-Bolaños, J.L., Botello-Álvarez, J.E., Martínez-González, G.M. and López-Isunza, F. (2009). Numerical study of natural convection in a 2-D square cavity with fluid-porous medium interface and heat generation. *Revista Mexicana de Ingeniería Química 8*, 169-185.

Lee, K. (2010). Simulation on the surfactant-polymer flushing of heterogeneous aquifers contaminated with non aqueous phase liquids. *Engineering Applications of Computational Fluid Mechanics 4*, 558-568.

Mikyška, J., Beneš, M. and Illangasekare, T. (2009). Numerical investigation of NAPL behavior at heterogeneous sand layers using VODA multiphase flow code. *Journal of Porous Media 12*, 685-694.

Niessner, J., Helmig, R., Jakobs, H. and Roberts, J. (2005). Interface condition and linearization schemes in the Newton iterations for two-phase flow in heterogeneous porous media. *Advances in Water Resources 28*, 671-687.

Kinjal, R., Manoj, N. and Twinkle, R. (2012). A mathematical model of imbibitions phenomenon in heterogeneous porous media during secondary oil recovery process. *Applied Mathematical Modelling*. doi: http://dx.doi.org/10.1016/j.apm.2012.06.015.

Salazar-Mendoza, R., Vázquez-Rodríguez, A., Ramos-Alcántara, J. R., Espinosa-Martínez, E. G. and Espinosa-Paredes, G. (2004). A two-region averaging model for solid-liquid flow with a moving bed in horizontal pipes. *Revista Mexicana de Ingeniería Química 3*, 273-286.

Schweizer, B (2008). Homogenization of degenerate two-phase flow equations with oil trapping. *SIAM Journal on Mathematical Analysis 39*. 1740-1763.

van Duijn, C., Molenaar, J. and de Neef, M. (1995). The effect of capillary forces on inmiscible two-phase flow in heterogeneous porous media. *Transport in Porous Media 21*, 71-93.